Available online at www.sciencedirect.com
ScienceDirect
Polymer 49 (2008) 546–553
polymer
www.elsevier.com/locate/polymer

Processing and characterization of electrospun poly(3-hydroxybutyrate-*co*-3-hydroxyhexanoate) nanofibrous membranes

Mei-Ling Cheng, Chih-Chung Lin, Hsiao-Lang Su, Po-Ya Chen, Yi-Ming Sun*

Department of Chemical Engineering and Materials Science, Yuan Ze University, Chung-Li 32003, Taiwan, ROC

Received 16 August 2007; received in revised form 20 November 2007; accepted 27 November 2007

Abstract

Poly(3-hydroxybutyrate-*co*-3-hydroxyhexanoate) (PHBHHx) nanofibrous membranes were first fabricated via electrospinning from chloroform ($CHCl_3$) or $CHCl_3$/dimethylformamide (DMF) polymer solutions. The electrospinning conditions such as the polymer concentration, the solvent composition, and the applied voltage were optimized in order to get smooth and nano-sized fibers. The crystalline structure, the melting behaviors and the mechanical properties of the obtained nanofibrous membranes were characterized. With pure $CHCl_3$ as the solvent in the electrospinning process, the finest smooth PHBHHx fibers were about 1 μm in diameter. When DMF is added to $CHCl_3$ as a co-solvent, the conductivity and volatility of the solution increased and reduced, respectively, and the electrospinnability of the polymer solution increased as a result. The averaged diameters of PHBHHx fibers could be reduced down to 300–500 nm when the polymer concentration was kept at 3 wt%, the ratio of DMF/$CHCl_3$ was maintained at 20/80 (wt%), and the applied voltage was fixed at 15 kV during electrospinning. WAXD and DSC results indicated that the crystallization of the PHBHHx nanofibers was restricted to specific crystalline planes due to the molecular orientation along the axial direction of the fibers. The crystallization behaviors of the electrospun nanofibers were significantly different from that of the cast membranes because of the rapid solidification and the one-dimensional fiber size effect in the electrospinning process. Mechanically, the electrospun PHBHHx nanofibrous membranes were soft but tough, and their elongation at break averaged 240–300% and could be up to 450% in some cases. This study demonstrated how the size of electrospun PHBHHx fibers could be reduced by adding DMF in the solvent and gave a clue of the presence of oriented molecular chain packing in the crystalline phase of the electrospun PHBHHx fibers.

Keywords: Electrospinning; Polyhydroxyalkanoates; Nanofibers

1. Introduction

Since it was introduced in the early 1930s, electrospinning has been actively explored due to its simplicity. It produces ultrafine polymer fibers with diameters typically in the range of several microns down to tens of nanometers. In this technique, polymer solution is drawn from a needle, forming a suspended droplet at the tip of the needle by force of gravity or mechanical pumping combined with electrostatic charge. A high-speed jet is formed in the outlet of the needle when the electrostatic charge overcomes the surface tension of the droplet, which in turn is splayed by the electric force. Solvents in the jet evaporate during the flight time, thus forming ultrafine fibers [1]. Electrospun nanofiber membranes have distinctive properties such as high surface area-to-volume ratio, high porosity, and enhanced specific mechanical performance, thus allowing for vast possibilities for surface functionalization. Electrospun nanofibrous membranes have been used in various applications such as nano-sensors, electronic/optical industrial applications, cosmetic skin masks, military body armor, filtration media, etc. [2]. Recently, many attempts in biomedical applications have been widely reported using biodegradable

* Corresponding author. Tel.: +886 3 4638800x2558; fax: +886 3 4559373.
E-mail address: cesunym@saturn.yzu.edu.tw (Y.-M. Sun).

0032-3861/$ - see front matter © 2007 Elsevier Ltd. All rights reserved.
doi:10.1016/j.polymer.2007.11.049

nanofibers as wound dressings, drug delivery systems [3], vascular grafts, and scaffolds for tissue engineering [4–6].

Polyhydroxyalkanoates (PHAs) are a class of biodegradable and biocompatible synthetic thermoplastic polyesters produced by various microorganisms as intracellular carbon and energy storage polymers [7–10]. Poly(3-hydroxybutyrate) (PHB), one of the most extensively studied species within the PHA family, is highly crystalline and rigid. For the purpose of industrial applications, its copolymer in various ratios with 3-hydroxyvalerate (HV), poly(3-hydroxybutyrate-*co*-3-hydroxyvalerate) (PHBV), was introduced to enhance the processing and mechanical properties of PHB. However, PHBV is a relatively unusual copolymer because HB and HV units are isodimorphous, that is, the HV units are incorporated into the PHB crystalline lattice [11]. Due to this isodimorphism, the characteristics of PHBV are not significantly improved in comparison to PHB homocopolymer. Copolymerization of PHB with longer chain hydroxyalkanoic acid, such as 3-hydroxyhexanoate (HHx), is designed to avoid the isodimorphism because HB and HHx components are unable to fit into the crystalline lattices of each other. The glass transition temperature (T_g) and melting temperature (T_m) of poly(3-hydroxybutyrate-*co*-3-hydroxyhexanoate) (PHBHHx) vary with the content of the HHx units present in the statistically random copolymer. The X-ray crystallinity decreases from 60% to 18% as the HHx fraction increases from 0 to 25 mol%. PHBHHx becomes soft and flexible with an increase in the HHx fraction. Thus, PHBHHx is superior to both PHB and PHBV in terms of mechanical and processing properties [12,13].

Non-woven biodegradable nanofibrous PHBV membrane has been prepared by electrospinning for tissue engineering. PHBV fibers were obtained by electrospinning from a PHBV/chloroform solution; resulting in an average fiber diameter of 2.5 μm. As an organosoluble salt (benzyl trialkylammonium chloride, BTEAC) was added to the electrospinning solution, the average fiber diameter was decreased to 1.0 μm; furthermore, the fibers linearized out from the swirled spaghetti-like arrangement [14]. PHBV nanofibrous membranes have also been fabricated by electrospinning then composited with hydroxyapatite (Hap) by soaking in simulated body fluid for use as scaffolds in tissue engineering [6]. The nanofibers fabricated from PHBV/2,2,2-trifluoroethanol (TFE) solution revealed a unimodal distribution of fiber diameters with an observed average diameter of 185 nm. Hap significantly enhanced the degradation rate of PHBV nanofibers in the presence of PHB depolymerase. Sombatmankhong et al. [15] studied the effect of electrospinning parameters on PHB, PHBV, and their blended fibers and obtained well-aligned, cross-sectionally round fibers by using a rotating cylindrical collector. The average diameter of the electrospun fibers from PHB and PHBV solutions ranged between 1.6 and 8.8 μm. Mechanically, much improvement in the tensile strength and the elongation at break was observed for the blended fiber membranes over those of the PHB and PHBV fiber ones. All the fibrous membranes exhibited better absorbance value in the indirect cytotoxic evaluation with mouse fibroblasts (L929) than tissue-culture polystyrene plate (TCPS); therefore, these membranes posed no threat to cells.

Previous reports showed that PHBHHx is flexible, tough and has better biocompatibilities with fibroblasts [16], chondrocytes [17], and nerve cells [18] than PHB and poly(lactic acid). However, to the best of our knowledge, there is no example of the fabrication of PHBHHx nanofibers by electrospinning in the literature. In this study, we demonstrate the first instance of a non-woven nanofibrous structure of PHBHHx prepared via electrospinning. The morphology of electrospun fibers depends on various parameters such as solution properties including viscosity and conductivity; processing variables including the applied electric voltage, feed rate, and tip-to-collector distance; ambient conditions including temperature, humidity, and air velocity in the electrospinning chamber, etc. Adjusting these parameters allows for the preparation of optimal ultrafine fibers. In order to explore the potentials of PHBHHx nanofibrous membranes in practical applications, the crystalline structure, thermal properties and mechanical properties are investigated.

2. Experimental

2.1. Materials

Poly(3-hydroxybutyrate-*co*-3-hydroxyhexanoate) (PHBHHx, with HHx content of 3.9% and 8.3%; named as PHBHHx4 and PHBHHx8, respectively) was obtained from Procter and Gamble (West Chester, OH, USA) as a gift ($\overline{M}_w$: PHBHHx4 = 967,000 g/mol and PHBHHx8 = 1,210,000 g/mol). Chloroform was from Mallinckrodt (Hazelwood, MO, USA). Dimethylformamide (DMF) was from Tedia (Fairfield, OH, USA).

2.2. Electrospinning process

The electrospinning instrument consisted of an adjustable, regulated, high-voltage power supply (up to 40 kV, You-Shang Technical Co., Taiwan), a syringe pump (Cole-Parmer, EK-74900-00, USA), and collector units. PHBHHx polymer was dissolved in chloroform or chloroform/dimethylformamide solution with desired concentrations. The polymer solution was filled in a glass syringe which was driven by the syringe pump. A positive high-voltage was applied through a wire to the tip of the syringe needle. In this arrangement, a strong electric field was created between the PHBHHx solution within the tip and the collector. When the electric field exceeded a critical value, mutual charge repulsion overcame the surface tension of the polymer solution and an electrically charged jet was ejected from the conical tip (called Taylor cone) of solution. Ultrafine fibers were collected on a flat aluminum foil connected to the ground under the syringe during the process. About 6 h processing time would be needed to produce a PHBHHx nanofibrous membrane with thickness of 70 μm. Electrospun membranes were carefully detached from the collector and dried in vacuum for 2 days to remove the solvent completely. In this study, the effects of polymer concentration in chloroform, co-solvent DMF addition, and the applied voltage between the tip and the collector were

investigated. The temperature was kept at 21 °C, the tip-to-collector distance was kept at 25 cm, and the feeding rate was kept at 0.5 ml/h during the operation of the electrospinning process.

As a reference sample, a cast membrane was prepared from a solution of 4 wt% PHBHHx in chloroform. The solution was cast on a glass plate and dried at room temperature. Finally, the membrane was dried in vacuum for 2 days.

2.3. Morphology of electrospun fibers

The collected fibers were observed by SEM (JEOL JSM-5600). Samples were mounted on metal stubs, and sputter-coated with gold for 40 s. The voltage of the apparatus was controlled at 20 kV. The morphology of electrospun fibers was observed from the SEM pictures. Moreover, the average diameter of electrospun fibers was measured by analyzing the SEM image. First, five horizontal straight lines were drawn on a SEM picture. All the diameters of the fibers which crossed the straight lines were measured. Finally, more than 250 data points were collected for the measurement of an average diameter of a kind of electrospun fibers.

2.4. Crystalline structure and crystallinity of membranes

The enthalpy of melting, ΔH_m, was measured by DSC (Perkin–Elmer DSC7, equipped with an intracooler). Samples were sealed in aluminum pans and weights of approximately 6 mg were used. Under a nitrogen atmosphere, samples were scanned from −40 °C to 180 °C with a rate of 10 °C/min. According to ΔH_m, the difference of crystallinity between the polymers in cast membranes and electrospun fibers could be determined.

Crystalline diffraction patterns were determined by a wide angle X-ray diffraction (WAXD, Shimadzu, XRD-600) generator operated at 40 kV and 30 mA. The diffraction angle was scanned from 2° to 40°, with a rate of 1°/min, under Cu radiation ($\lambda = 0.1542$ nm).

2.5. Mechanical test

Mechanical properties in terms of tensile strength, Young's modulus, elongation at break, and toughness were measured by using an Instron tester (model 4204). The gauge length and crosshead speed are 50 mm and 10 mm min^{-1}, respectively. All samples were prepared in the form of standard dumbbell-shaped according to ASTM D638 by die cutting (DIN 53504-S3A, Shimadzu, Japan). The total length and neck width of the dumbbell-shaped membrane sheet are 50 mm and 4 mm, respectively. The apparent thickness of the membrane was determined by a digital thickness gauge (Mitutoyo, IDF-112) in an average of 10 measures at different points of the membrane. The apparent thicknesses of electrospun nanofibrous membranes are 65 ± 9 and 87 ± 10 μm for PHBHHx4 and PHBHHx8, respectively. For the cast membranes, the thickness is 50 ± 10 μm. Obtained results were averaged over five samples for each condition.

3. Results and discussion

3.1. The effect of polymer concentration

Polymer concentration directly affects the quality of electrospun fibers. Fig. 1 shows the SEM pictures of electrospun PHBHHx fibers prepared from the polymer/chloroform solutions with different polymer concentrations. At lower polymer concentrations, bead fibers formed. Smooth fibers of PHBHHx4 and PHBHHx8 were not formed until polymer concentrations exceeded 5 and 4 wt%, respectively. The lower viscosity of the PHBHHx solution at lower polymer concentrations is a likely reason leading to bead fiber formation. As polymer concentrations increased, the solution viscosities increased (Fig. 2) because the entanglement of polymer molecular chains prevented the breakup of the electrically driven jet and allowed the electrostatic stresses to further elongate the jet; thus the formation of smooth fibers was more favored than that of beaded fibers [19,20].

3.2. The effect of DMF

When chloroform alone was used as the solvent for the electrospinning of PHBHHx, the needle tip was easily blocked at high polymer concentrations due to solvent evaporation. To compensate, DMF was used to lower solvent volatility (the boiling point of DMF is 153 °C, whereas that of chloroform is 61.2 °C); incidentally, on addition of DMF co-solvent to the 3 wt% PHBHHx polymer solution smooth fibers formed instead of beaded fibers. The SEM pictures of the fibers prepared with DMF/$CHCl_3$ are shown in Fig. 3. As DMF concentration increased, bead fibers changed to smooth fibers and the fiber diameters decreased (Tables 1 and 2). As shown in Fig. 4, the viscosity of the polymer solution actually decreased with increased concentration of the co-solvent DMF. In fact, the viscosities in which smooth fibers began to form in paired DMF/$CHCl_3$ solution were nearly half that of chloroform. The reduction of viscosities indicates that the solubility of PHBHHx in the solution decreases as the poor solvent DMF is added. In chloroform alone, the PHBHHx solution had a lower viscosity, which led to bead fiber morphology (see Section 3.1) and smaller fiber diameter. However, the addition of co-solvent DMF tended to enhance the electrospinnability of PHBHHx polymer. Electrospinnability indicates the chance of a given polymer–solvent system being able to eject continuous fibers out from a needle tip [21]. Lee et al. [22] indicated that the high dielectric constant of DMF might contribute significantly to the reduction in the diameter of the jet. Dielectric constants at 20 °C for chloroform and DMF are reported to be 4.8 and 36.7, respectively [23]. As shown in Fig. 4, the addition of DMF increased the conductivity of the solution. The higher conductivity would lead to a higher charge capacity of the solution, which in turn increased the stretching force on the jet splay [18]. Even at lower polymer concentrations, the stretching force of the jet splay was enhanced, allowing for the reduction of fiber diameters and formation of bead fibers. Furthermore, the reduction of solvent volatility via

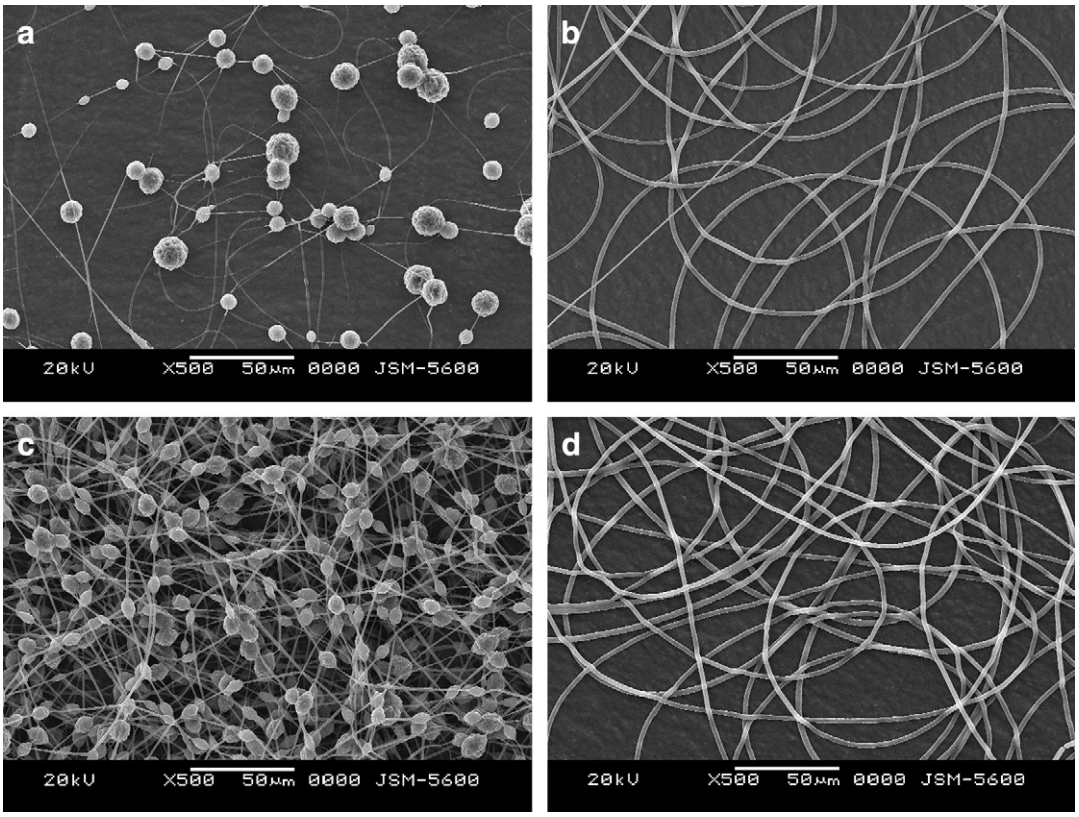

Fig. 1. The effect of polymer concentration on the morphology of the electrospun PHBHHx4 fibers: (a) 2 and (b) 5 wt%; the electrospun PHBHHx8 fibers: (c) 2 and (d) 4 wt% (9 kV, $CHCl_3$).

the addition of DMF led to an increase of stretching time while the jet splayed, and it allowed further fiber extension and resulted in the formation of smooth fibers. Combining the effects of conductivity, volatility, and viscosity of the polymer solution on the morphology of PHBHHx fibers, it can be concluded that the addition of DMF in the solution would enhance the electrospinnability and it was highly effective for producing smooth nano-sized fibers in the electrospinning process for PHBHHx polymers.

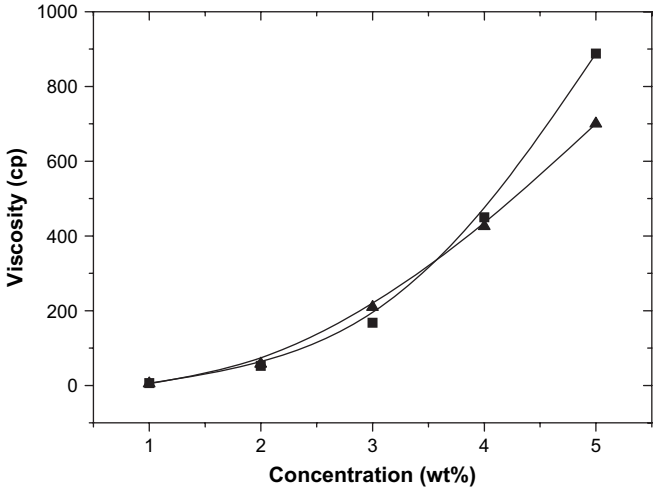

Fig. 2. The relationship of viscosity and polymer concentration: (■) PHBHHx4 and (▲) PHBHHx8 ($CHCl_3$).

3.3. The effect of applied voltage

As shown in Fig. 5, fiber diameters decreased as the applied voltage increased. Higher voltages led to a stronger electric field, columbic force, and stretching force on the jet splay, which further reduced fiber diameters [20,24,25]. Increasing voltages from 9 to 15 kV decreased the average PHBHHx4 nanofiber diameters significantly; yet, further increments in voltage above 15 kV did not result in any significant variation in average PHBHHx4 nanofiber diameters. When applied voltages exceeded 18 and 15 kV for PHBHHx4 and PHBHHx8, respectively, the distribution of nanofiber diameters broadened because the higher applied voltages (columbic force) unbalanced the jet splay's viscous interaction and surface tension [3,26], hence destabilizing the Taylor cone and leading to less control of the fiber diameter distribution. Thus, even though there was only a slight decrease in fiber diameter at 18 kV for PHBHHx4, there was a better quality control than that at other voltages. Whereas the diameters of PHBHHx8 presented a near inverse linear relationship with the applied voltage, there was little difference; but, the stability and control of the Taylor cone was optimal at 15 kV. Therefore, the nanofibers prepared for further characterizations were obtained with 18 and 15 kV for PHBHHx4 and PHBHHx8, respectively, while the polymer concentration was kept at 3 wt% and the ratio of DMF/$CHCl_3$ was maintained at 20/80 (wt%). Under these conditions, the average diameters of the PHBHHx4 and PHBHHx8 nanofibers spun were 340 and 490 nm, respectively.

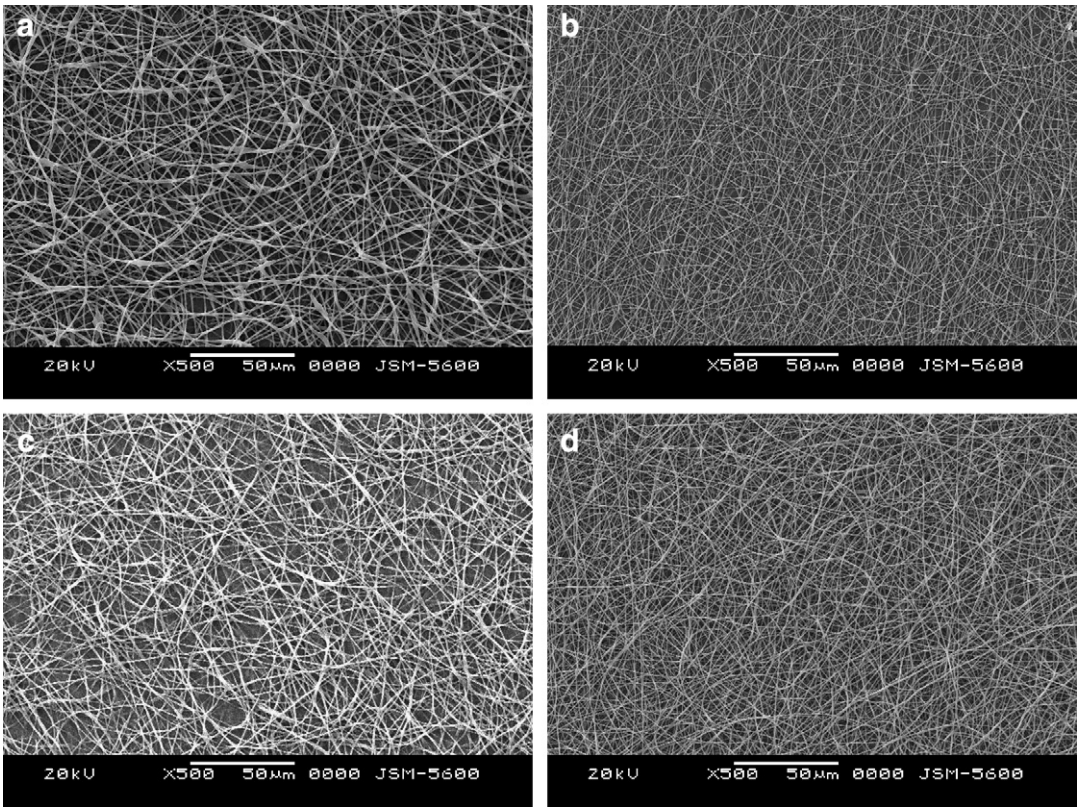

Fig. 3. The effect of DMF concentration on the morphology of the electrospun fibrous membranes: PHBHHx4 with DMF content of (a) 5 and (b) 20 wt%; PHBHHx8 with DMF content of (c) 5 and (d) 20 wt% in the DMF/$CHCl_3$ solution (3 wt% polymer, 9 kV).

Table 1
The effect of DMF concentration in the DMF/$CHCl_3$ solution on the morphology and fiber diameters of the as-spun PHBHHx4 fibers (3 wt% polymer, 9 kV)

DMF (wt%)	Morphology	Fiber diameters (nm)
0	Bead fiber	–
5	Bead fiber	–
10	Bead fiber	–
15	Fiber	650 ± 120
20	Fiber	640 ± 100

Table 2
The effect of DMF concentration in the DMF/$CHCl_3$ solution on the morphology and fiber diameters of the as-spun PHBHHx8 fibers (3 wt% polymer, 9 kV)

DMF (wt%)	Morphology	Fiber diameters (nm)
0	Bead fiber	–
5	Fiber	1000 ± 70
10	Fiber	840 ± 110
15	Fiber	730 ± 90
20	Fiber	430 ± 150

3.4. The crystalline structure and melting behaviors of the fibers

The crystalline properties of the electrospun fibers are important in practical application. PHB homopolymer is a hard and brittle material due to its high crystallinity. When a small amount of 3-hydroxyhexanoate is randomly incorporated into PHB, the 3-hydroxyhexanoate monomers act as impurities and are excluded from the PHB crystalline lattice [27]. WAXD spectra of PHBHHx electrospun membranes are compared with that of PHBHHx cast membranes as shown in Fig. 6. The WAXD spectra of PHBHHx cast membranes showed similar results as that of PHB and PHBHHx spectra reported in the literature [12,27]. The electrospun PHBHHx fibers presented only two crystalline peaks on the (020) and (110) reflection planes, whereas all the other crystalline peaks disappeared. The size effect of one-dimensional fibers may restrain

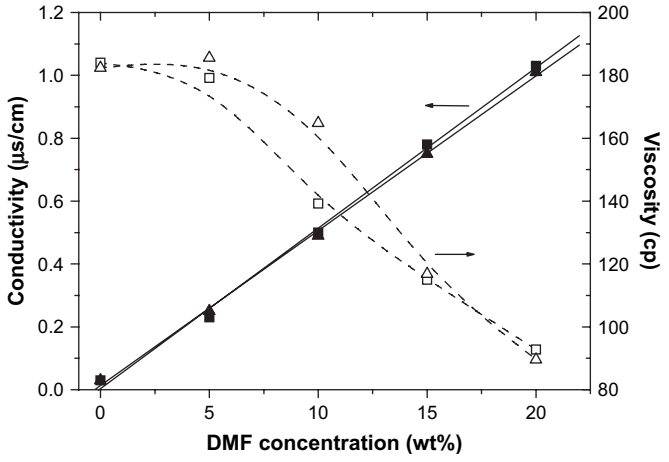

Fig. 4. The relationships of conductivity (—, solid symbol) and viscosity (- - -, empty symbol) and the DMF concentration in the DMF/$CHCl_3$ solution: (■, □) PHBHHx4 and (▲, △) PHBHHx8 (3 wt% polymer).

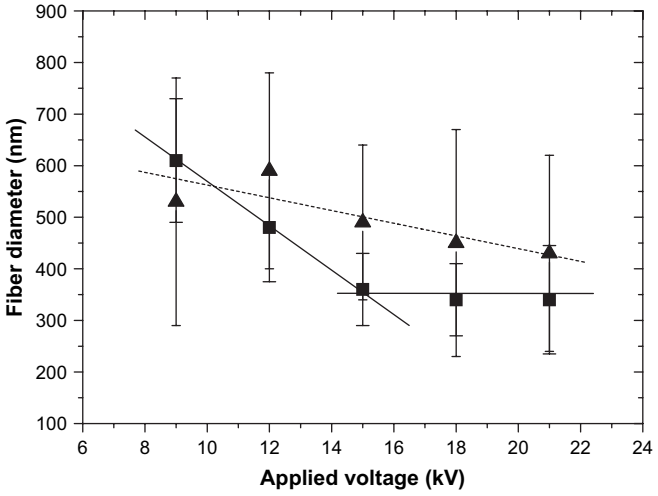

Fig. 5. The relationship of fiber diameters and applied voltage: (■) PHBHHx4, (▲) PHBHHx8, (—) linear fit for PHBHHx4, and (- - -) linear fit for PHBHHx8 (3 wt% polymer, DMF/$CHCl_3$ = 20/80 wt%).

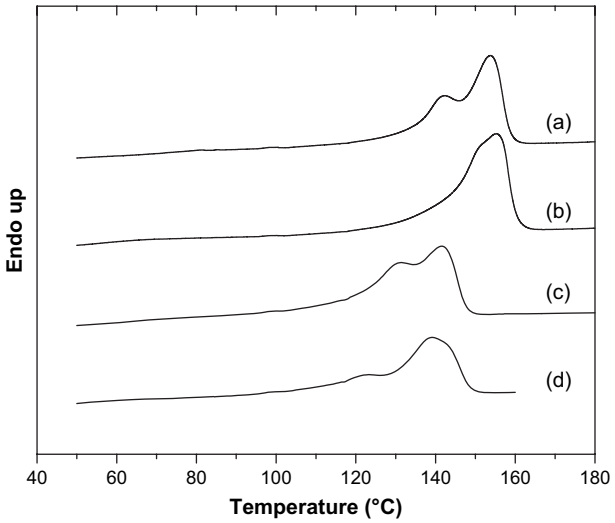

Fig. 7. DSC thermograms of various membranes: (a) cast PHBHHx4, (b) electrospun PHBHHx4, (c) cast PHBHHx8, and (d) electrospun PHBHHx8.

crystal growth on the other reflection planes. In addition, the (110) diffraction peak of electrospun fibers was sharper and stronger than that of the cast membranes. This indicated that both the (110) reflection plane and the fibers themselves have a molecular orientation along the fiber axis (*c*-axis). There was oriented chain packing in the crystalline phase of the electrospun PHBHHx fibers.

Fig. 7 illustrates the DSC thermograms of PHBHHx nanofibers and cast membranes. Two melting peaks are observed on the melting curve of PHBHHx cast membranes. The multiple melting peaks of semicrystalline polymers can be attributed to compositional heterogeneity, multiple crystalline forms, or simply from recrystallization during the heating run. For PHBHHx with 3-hydroxyhexanoate content lower than 18 mol%, the lower temperature peak is a real melting point (T_m) of the crystal formed originally, while that at higher temperatures is the melting peak of the crystal formed by recrystallization during the DSC heating process [28–30]. However, the PHBHHx electrospun fibrous membranes have only one melting peak on the melting curve. In order to determine the melting behavior of electrospun fibers, DSC measurements at different heating rates were carried out for the samples. The results, shown in Table 3, indicate that the overall melting enthalpy increases with decreasing heating rate. It seems that the copolymer chains have enough time to rearrange to be better crystal packing at lower DSC heating rates because rapid solidification of stretched chains at high elongational rates during the later stages of electrospinning hindered the formation of large crystals. The crystalline stack of electrospun fibers was restricted to the *c*-axis alone, the formation of crystallites during solidification was limited and no spherulitic structure was presented. The crystallites gradually melt during the heating scan and the observed peak is only a result of melting of the recrystallized crystallites formed during the heating scan. In addition, the rapid solidification and restricted crystalline structure of electrospun fibers resulted in smaller melting heats than the melting heats of cast membranes (Table 3).

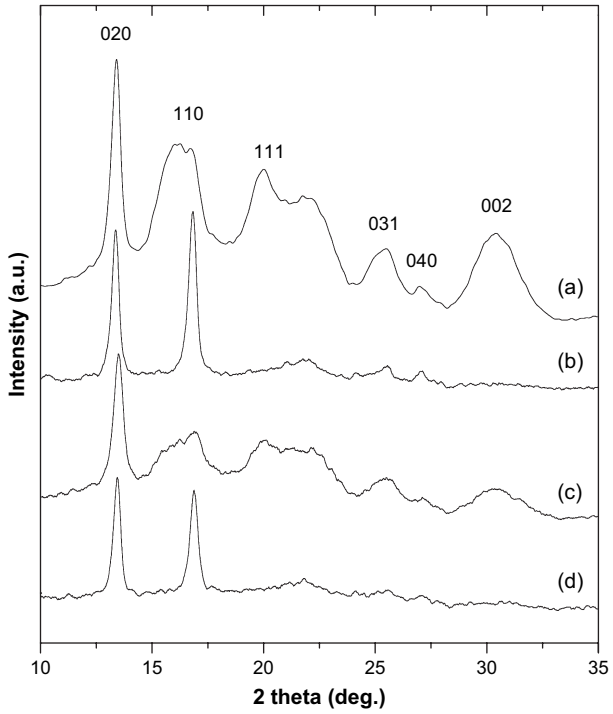

Fig. 6. WAXD spectra of various membranes: (a) cast PHBHHx4, (b) electrospun PHBHHx4, (c) cast PHBHHx8, and (d) electrospun PHBHHx8.

3.5. Mechanical properties of the membrane

The mechanical behaviors of electrospun nanofibrous membranes and cast membranes are significantly different. Stress–strain curves of these membranes are shown in Fig. 8. In contrast to the hard and brittle cast membranes, electrospun nanofibrous membranes are soft but tough. The Young's modulus, elongation at break, tensile strength, and toughness of electrospun fibrous membranes and cast membranes are summarized in Table 4. The electrospun nanofibrous membranes had lower Young's modulus, lower tensile strength, higher elongation at

Table 3
The thermal properties of the cast and electrospun PHBHHx membranes from DSC study

Scanning rate (°C/min)	PHBHHx4					PHBHHx8				
	Cast			Electrospun		Cast			Electrospun	
	T_{m1} (°C)	T_{m2} (°C)	ΔH_m (J/g)	T_m (°C)	ΔH_m (J/g)	T_{m1} (°C)	T_{m2}(°C)	ΔH_m (J/g)	T_m (°C)	ΔH_m (J/g)
5	139.5	151.9	65.0	150.7	62.9	129.1	140.0	48.0	138.6	51.9
10	142.3	153.7	61.3	155.2	59.8	131.3	141.5	48.3	139.2	45.1
20	146.0	153.3	60.9	152.7	57.8	132.0	141.0	46.8	142.7	44.9
40	–	155.3	64.9	154.7	53.2	–	141.3	47.2	141.3	42.9

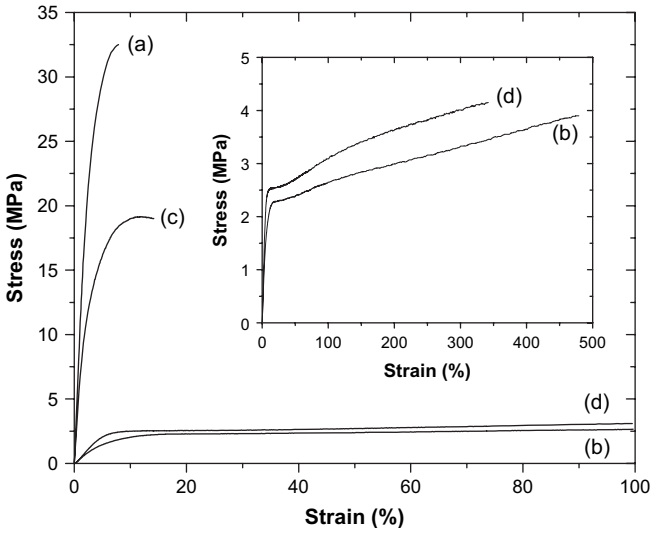

Fig. 8. The stress–strain curve of various membranes: (a) cast PHBHHx4, (b) electrospun PHBHHx4, (c) cast PHBHHx8, and (d) electrospun PHBHHx8. (The inset is an overall diagram for the samples (b) and (d).)

break, and higher toughness than the cast membranes. The tensile strength of the electrospun nanofibrous membranes was largely reduced due to the absence of solid domains. Nevertheless, the polymer molecular chains are oriented uniformly along the fiber axis. The elongation at break of electrospun PHBHHx4 membranes averaged 300% and could reach as high as 450% in some cases. In cast membranes, the addition of more 3-hydroxyhexanoate components into PHBHHx copolymer reduced the Young's modulus and tensile strength but increased the elongation at break due to lowered crystallinity. In electrospun nanofibrous membranes, increased 3-hydroxyhexanoate content did not seem to affect the mechanical properties probably because the effect of the non-uniform fiber diameters became greater than the effect of 3-hydroxyhexanoate content. However, this could also be the result of using the "apparent" cross-sectional area, as the true cross-sectional area of all the fibers at the neck of the test samples was not available for the calculation of tensile strength.

Table 4
The mechanical properties of the cast and electrospun PHBHHx membranes

	Membrane	Young's modulus (GPa)	Elongation (%)	Toughness (J/m^3)	Tensile strength (MPa)
PHBHHx4	CA*	0.8 ± 0.2	6 ± 1	120 ± 60	25 ± 9
	ES	0.025 ± 0.009	300 ± 150	1000 ± 350	4.1 ± 0.5
PHBHHx8	CA	0.5 ± 0.2	14.5 ± 0.8	190 ± 50	16 ± 4
	ES	0.035 ± 0.005	240 ± 70	720 ± 270	3.5 ± 0.6

* CA: cast membrane, ES: electrospun membrane.

According to Sombatmankhong et al. [15], the tensile strength of electrospun PHB and PHBV nanofibrous membranes were found to be 1.6 and 1.8 MPa, respectively, and the elongation at break of the electrospun PHB, PHBV, and PHB/PHBV blended nanofibrous membranes were in the range of 2–7%, which were similar to that of our PHBHHx cast membranes. In our study, electrospun PHBHHx nanofibrous membranes showed enormous enhancement of the elongation at break (ranged from 200% to 450%) and the tensile strength (ranged from 3 to 4.5 MPa). The flexible and tough electrospun PHBHHx nanofibrous membranes might be useful in various applications, such as tissue engineering, drug delivery carrier, wound dressing, etc.

4. Conclusion

In this study, it has been demonstrated that the nanofibers of biodegradable PHBHHx polymer could be fabricated by the electrospinning technique. The solution properties such as viscosity, volatility and conductivity correlated strongly with the morphology of electrospun nanofibrous membranes. In order to customize fiber diameters, process parameters such as polymer solution concentration, co-solvent weight ratio, and applied voltage in electrospinning process could be adjusted. Polymer concentration of PHBHHx4 and PHBHHx8 in chloroform alone must exceed 5 and 4 wt%, respectively, in order to obtain the smooth fibers. When DMF was added as co-solvent, smooth fibers formed even at low polymer concentrations and the fiber diameters decreased with the increase of the fraction of DMF in the solution. In addition, an increase in the applied voltage caused a decrease in the average diameter of nanofibers. Ultrafine PHBHHx fibers with a minimal average diameter of 340 nm were obtained.

The electrospun PHBHHx nanofibers presented two strong crystalline planes as indicated in WAXD analysis. The molecular orientation of the chain packing along the fiber axis has been demonstrated. Due to the one-dimensional fiber size effect, the growth of crystalline phase on the radial direction of the fibers was restrained. The melting heat of the electrospun nanofibrous membranes was smaller than that of the cast membranes by the reason of rapid solidification and restricted crystalline structure. Mechanically, great improvement of the elongation at break was observed for the electrospun PHBHHx nanofibrous

membranes. The application of these PHBHHx nanofibrous membranes as scaffolds in tissue engineering will be a focus in our future investigations.

Acknowledgments

This work was supported by the National Science Council of the Republic of China through the grants of NSC95-2622-E-155-001 and NSC95-2218-E-155-001. The authors would like to thank Dr. Isao Noda of the Procter and Gamble Co. for his kind supply of PHBHHx samples and Mr. Jeffrey F. Hsu of the Department of Chemistry, University of Missouri at Kansas City for his kind assistance in editing this manuscript.

References

[1] Jaeger R, Bergshoef MM, Batlle CM, Schoönherr H, Vancso GJ. Macromol Symp 1998;127:141.
[2] Huang ZM, Zhang YZ, Kotaki M, Ramakrishna S. Compos Sci Technol 2003;63:2223.
[3] Katti D, Robinson KW, Ko FK, Laurencin C. J Biomed Mater Res Part B Appl Biomater 2004;70B:286.
[4] Li WJ, Laurencin CT, Caterson EJ, Tuan RS, Ko FK. J Biomed Mater Res 2002;60:613.
[5] Yoshimoto H, Shin YM, Terai H, Vacanti JP. Biomaterials 2003;24:2077.
[6] Ito Y, Hasuda H, Kamitakahara M, Ohtsuki C, Tanihara M, Kang IK, et al. J Biosci Bioeng 2005;100:43.
[7] Rhie HG, Dennis D. Appl Environ Microbiol 1995;61:2487.
[8] Wong HH, Lee SY. Appl Microbiol Biotechnol 1998;50:30.
[9] Ahn WS, Park SJ, Lee SY. Appl Environ Microbiol 2000;66:3624.
[10] van Wegen RJ, Lee SY, Middelberg AP. Biotechnol Bioeng 2001;74:70.
[11] Yoshie N, Saito M, Inoue Y. Macromolecules 2001;34:8953.
[12] Doi Y, Kitamura S, Abe H. Macromolecules 1995;28:4822.
[13] Asrar J, Valentin HE, Berger PA, Tran M, Padgette SR, Garbow JR. Biomacromolecules 2002;3:1006.
[14] Choi JS, Lee SW, Jeong L, Bae SH, Min BC, Youk JH. Int J Biol Macromol 2004;34:249.
[15] Sombatmankhong K, Suwantong O, Waleetorncheepsawat S, Supaphol P. J Polym Sci Part B Polym Phys 2006;44:2923.
[16] Yang XS, Zhao K, Chen GQ. Biomaterials 2002;23:1391.
[17] Zhao K, Deng Y, Chen JC, Chen GQ. Biomaterials 2003;24:1041.
[18] Yang M, Zhu SS, Chen Y, Chang ZJ, Chen GQ, Gong YD, et al. Biomaterials 2004;25:1365.
[19] Mit-uppatham C, Nithitanakul M, Supaphol P. Macromol Chem Phys 2004;205:2327.
[20] Buchko CJ, Chen LC, Shen Y, Martin DC. Polymer 1999;40:7397.
[21] Pattamaprom C, Hongrojjanawiwat W, Koombhongse P, Supaphol P, Jarusuwannapoo T, Rangkupan R. Macromol Mater Eng 2006;291:840.
[22] Lee K, Kim H, Khil M, Ra Y, Lee D. Polymer 2003;44:1287.
[23] Lide David R, editor. Handbook of chemistry and physics. 73rd ed. Boca Raton, FL: CRC Press; 1993.
[24] Megelski S, Stephens JS, Chase DB, Rabolt JF. Macromolecules 2002;35:8456.
[25] Lee JS, Choi KH, Ghim HD, Kim SS, Chun DH, Kim HY. J Appl Polym Sci 2004;93:1638.
[26] Supaphol P, Wannatong L, Sirivat A. Polym Int 2004;53:1851.
[27] Sato H, Nakamura M, Padershoke A, Yamaguchi H, Terauchi H, Ekgasit S, et al. Macromolecules 2004;37:3763.
[28] Yoshie N, Menju H, Sato H, Inoue Y. Macromolecules 1995;28:6516.
[29] Watanabe T, He Y, Fukuchi T, Inoue Y. Macromol Biosci 2001;1:75.
[30] Chen C, Cheung MK, Yu PHF. Polym Int 2005;54:1055.